AD-A194 489 HIGH PERFORMANCE CHARGE TRANSFER DEVICE DETECTORS(U) 1/1
ARIZONAUUNIV TUCSON DEPT OF CHEMISTRY
J V SWEEDLER ET AL 04 FE 88 TR-64 N00014-86-K-0316
UNCLASSIFIED F/G 9/1 NL

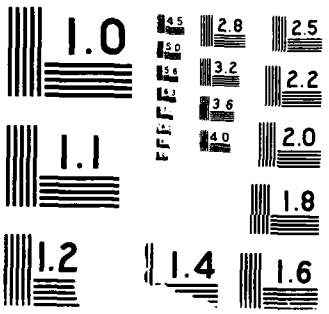
1.0
1.1
1.2
1.4
1.6
1.8
2.0
2.2
2.5
2.8
3.2
3.6
4.0
4.5
5.0
5.6

UNCLASSIFIED

REPORT DOCUMENTATION PAGE

AD-A194 409

DTIC ELECTE APR 25 1988 S D

DTIC FILE COPY

1b. RESTRICTIVE MARKINGS	
2b. DECLASSIFICATION / DOWNGRADING SCHEDULE	3. DISTRIBUTION / AVAILABILITY OF REPORT: Approved for public release; distribution unlimited
4. PERFORMING ORGANIZATION REPORT NUMBER(S): 64	5. MONITORING ORGANIZATION REPORT NUMBER(S)
6a. NAME OF PERFORMING ORGANIZATION: University of Arizona	6b. OFFICE SYMBOL (If applicable)
7a. NAME OF MONITORING ORGANIZATION: Office of Naval Research	
6c. ADDRESS (City, State, and ZIP Code): Department of Chemistry, Tucson, Arizona 85721	7b. ADDRESS (City, State, and ZIP Code): Arlington, Virginia 22217
8a. NAME OF FUNDING / SPONSORING ORGANIZATION: Office of Naval Research	8b. OFFICE SYMBOL (If applicable)
9. PROCUREMENT INSTRUMENT IDENTIFICATION NUMBER: N00014-86-K-0316	
8c. ADDRESS (City, State, and ZIP Code)	10. SOURCE OF FUNDING NUMBERS: PROGRAM ELEMENT NO. / PROJECT NO. / TASK NO. / WORK UNIT ACCESSION NO.

11. TITLE (Include Security Classification)
"High Performance Charge Transfer Device Detectors"

12. PERSONAL AUTHOR(S)
J.V. Sweedler, R.B. Bilhorn, P.M. Epperson, G.R. Sims, and M.B. Denton

13a. TYPE OF REPORT	13b. TIME COVERED	14. DATE OF REPORT (Year, Month, Day)	15. PAGE COUNT
Technical	FROM 5/15/86 TO 4/30/89	February 4, 1988	31

16. SUPPLEMENTARY NOTATION
Submitted to Analytical Chemistry for publication

17. COSATI CODES		
FIELD	GROUP	SUB-GROUP

18. SUBJECT TERMS (Continue on reverse if necessary and identify by block number)
Charge transfer devices, charge-coupled devices, charge injection devices, multichannel techniques, spectroscopic detectors, electro-optical performance

19. ABSTRACT (Continue on reverse if necessary and identify by block number)

This article is the first in a two-part series describing charge transfer devices (CTDs) -- a relatively new class of multichannel detectors for the ultraviolet to near-infrared spectral regions. An overview of the operation and the characteristics of CTDs relevant to analytical spectroscopy is presented. The sensitivity and dynamic range obtainable from CTD detectors are discussed and compared to the sensitivity and dynamic range obtainable from other spectroscopic detectors. Unique capabilities such as the ability to nondestructively readout the detector array and the ability to alter the effective detector element size using the process of binning are described. Detector array formats ranging from single elements to extremely large arrays, large photoactive areas, high quantum efficiencies, dark count rates allowing long integration times and low read noises all contribute to the outstanding performance and great flexibility offered by CTDs.

20. DISTRIBUTION / AVAILABILITY OF ABSTRACT	21. ABSTRACT SECURITY CLASSIFICATION
☒ UNCLASSIFIED/UNLIMITED ☐ SAME AS RPT. ☐ DTIC USERS	UNCLASSIFIED

22a. NAME OF RESPONSIBLE INDIVIDUAL	22b. TELEPHONE (Include Area Code)	22c. OFFICE SYMBOL
M. Bonner Denton	(602) 621-6352	

FORM 1473, 84 MAR — 83 APR edition may be used until exhausted. All other editions are obsolete.

SECURITY CLASSIFICATION OF THIS PAGE
UNCLASSIFIED

OFFICE OF NAVAL RESEARCH

Contract N00014-86-K-0316

R&T Code 4131012---03

Technical Report No. 64

High Performance Charge Transfer Device Detectors

by

Jonathan V. Sweedler, Robert B. Bilhorn, Patrick M. Epperson,
Gary R. Sims, and M. Bonner Denton

Prepared for Publication in

Analytical Chemistry

Department of Chemistry
University of Arizona
Tucson, Arizona 85721

February 4, 1988

HIGH PERFORMANCE CHARGE TRANSFER DEVICE DETECTORS

J.V. Sweedler, R.B. Bilhorn, P.M. Epperson,
G.R. Sims, and M.B. Denton

Department of Chemistry
University of Arizona
Tucson, AZ 85721

Index Headings: Charge transfer devices, charge-coupled devices, charge injection devices, multichannel techniques, spectroscopic detectors, electro-optical performance

ABSTRACT

This article is the first in a two-part series describing charge transfer devices (CTDs)-- a relatively new class of multichannel detectors for the ultraviolet to near-infrared spectral regions. An overview of the operation and the characteristics of CTDs relevant to analytical spectroscopy is presented. The sensitivity and dynamic range obtainable from CTD detectors are discussed and compared to the sensitivity and dynamic range obtainable from other spectroscopic detectors. Unique capabilities such as the ability to nondestructively readout the detector array and the ability to alter the effective detector element size using the process of binning are described. Detector array formats ranging from single elements to extremely large arrays, large photoactive areas, high quantum efficiencies, dark count rates allowing long integration times and low read noises all contribute to the outstanding performance and great flexibility offered by CTDs.

High Performance Charge Transfer Device Detectors

Jonathan V. Sweedler, Robert B. Bilhorn, Patrick M. Epperson,

Gary R. Sims, and M. Bonner Denton

Department of Chemistry

University of Arizona

Tucson, Arizona 85721

Numercus modern analytical techniques are based on detection and quantitation of light in the ultraviolet to near infrared regions of the spectrum. Sensitive atomic and molecular spectroscopies including luminescence, absorption, emission and Raman require detectors with high responsivity, low read noise, large dynamic range, low dark count rate, and a linear or well-behaved response. Revolutionary developments in multichannel detectors have greatly expanded and improved the capabilities of current spectrochemical techniques.

There is great interest in replacing single channel photomultiplier tubes with multichannel devices (1,2). Multichannel detectors such as vidicons, intensified target vidicons, image dissectors, and photodiode arrays (PDAs) do not offer the sensitivity, dynamic range and noise performance necessary to be competitive with the PMT in many situations. Successful application of these multichannel detectors is limited to experimental conditions where the multichannel advantage outweighs the noise, crosstalk and dynamic range disadvantages.

New multichannel alternatives to PMT detection are finally capable of superior sensitivity and dynamic range, when compared on a detector element by detector element basis. In fact, some of these devices exceed the sensitivity and dynamic range of all other available detectors. The performance of charge transfer devices (CTDs) has advanced to the point where the application of this technology to the field of analytical chemistry is appropriate. In the first part of this two-part series, the theory, design, operation and performance of CTD detectors are described. The second article focuses on a range of analytical applications.

CTDs are solid-state multichannel detectors. These detectors integrate signal information as light strikes them, much like photographic film. An individual detector in a CTD array consists of several conductive electrodes overlying an insulating layer forming a series of metal-oxide-semiconductor (MOS) capacitors. The insulator separates the electrodes from a doped silicon region used for photogenerated charge storage. The actual geometry of the electrodes and insulators varies depending on the device and manufacturer. The basic operation of a CTD detector element can be illustrated by considering the simple example shown in Figure 1 depicting the cross section of a single detector element made from n-doped silicon. In this n-doped silicon, the majority current carrier is the electron, and the minority carrier is the hole. When the electrodes are negatively charged with respect to the silicon, a charge inversion region is created under the electrodes. This charge inversion region is an energetically favorable location for mobile holes to reside. The promotion of an electron into the semiconductor conduction band, such as by the absorption of a photon, creates a mobile hole that migrates to and is collected in the inversion region. In Figure 1, one electrode is held at a more negative potential than the other, making the accumulation of positive charge more favorable under this electrode.

The amount of charge generated in a CTD detector is measured either by moving the charge from the detector element where it is collected to a charge sensing amplifier or by moving it within the detector element and measuring the voltage change induced by this movement. These two modes of charge sensing are employed by the charge-coupled device (CCD) and the charge injection device (CID), respectively. While CTDs made of n-doped silicon (commonly employed in CIDs) collect photogenerated holes, and CTDs made from p-doped

silicon (commonly employed in CCDs) collect photogenerated electrons, by convention the photogenerated charge is always referred to in units of electrons. Complete descriptions of the operation of particular sensors appear in the optical engineering literature and are now beginning to appear in the chemical literature (see for example refs. 1-7).

In the CCD, the charge from each detector element is shifted in sequence to an amplifier located at the end of a linear or corner of a two dimensional array of detector elements. Charge is transferred to the on-chip amplifier by sequentially passing the charge packets from one detector element to the next adjacent detector element. A series of electrodes in each detector element are used to perform this transfer. The number of independent electrodes used to affect this transfer range from one to four, giving rise to CCDs appropriately called uniphase to four-phase devices (6,7). The potentials of the electrodes in a detector element provide a barrier that separates adjacent charge packets. Shifting the location of this barrier in a controlled manner causes charge to migrate in the desired direction. CCDs differ from other detectors by their ability to transfer the photogenerated signal from the photoactive element to an on-chip amplifier. This amplifier allows the CCD to obtain a very high signal-to-noise output. While digitization of the data in all CCD detector elements is not necessary, the architecture of the CCD requires shifting through the entire detector before proceeding to the next exposure; thus subarrays may not be randomly read in CCD detectors.

The organization of a two dimensional 3-phase CCD array is illustrated in Figure 2. Columns are clocked in parallel. With each clock, all of the charge in the imaging array is shifted toward the serial register by one row, while charge from the row adjacent to the serial register is transferred into

the serial register. Once the charge is shifted into the serial register, the charge packets are shifted sequentially to the on-chip amplifier. The illumination of the CCD must be minimized during the charge transfer readout process to prevent blurring of the image. Fixed potential barriers between columns separate charge from adjacent columns. Extremely efficient transfer of charge from detector element to detector element is critical since even small losses (on the order of 0.0001% loss per transfer) accumulate and become significant after the thousands of transfers required to read large CCDs. Modern CCDs are capable of thousands of charge transfers with almost immeasurable charge transfer losses (8,9).

A CID detector element consists of the intersection of two crossed electrodes. The electrodes are termed the collection electrode and the sense electrode. An array of collection and sense electrodes form a network that allows addressing individual detector elements. Charge is kept in the detector element by potential barriers which prevent the photogenerated charge from migrating along the electrodes. Any individual CID detector element can be read by transferring the charge from under the collection electrode to the sense electrode and measuring the voltage change this induces on the sense electrode. Since this readout process does not alter the charge contained within the element, the process has been termed the non-destructive readout mode (1,10). Charge is cleared from a detector element by applying the substrate voltage to both electrodes, which injects the charge into the bulk silicon.

CIDs are fabricated to allow random access of any given detector element using high speed shift registers for addressing. These registers connect the collection and sense electrodes to the drive signal and output amplifier

respectively, as shown in Figure 3. The integrated signal at the intersection of the selected collection and sense electrodes is either read using the nondestructive readout process or cleared using charge injection.

Format

The detector should not limit a spectroscopic system, rather the ideal detector should be available in the correct physical format and size. Although not optimally configured for many current spectroscopic systems, CTDs are available with a wide variety of photoactive areas and number of detector elements. Figure 4 shows a collection of CTDs demonstrating their wide range of photoactive areas and formats. Table I describes the characteristics of a variety of CTDs. The large number of detector elements available with some of the CTDs allows extremely high resolution spectra to be obtained simultaneously. For example, an echelle spectrometer used in conjunction with a rectangular CTD containing several hundred thousand detector elements is able to cover the ultraviolet, visible and near infrared spectral regions with greater than 0.01 nm resolution (11). Because of the large variety of available detectors, a CTD often can be selected for a specific application matching the number of detector elements and device performance to experimental requirements. The relative small size of the individual detector elements in most CTDs is a significant problem which requires ingenuity in optical design (2). The second article in this series describes a variety of spectroscopic systems which effectively utilize these detectors.

Detector Noise

A properly designed photon counting PMT is able to detect individual photoelectrons; i.e., essentially no noise is associated with the actual readout of this detector. For integrating detectors, the situation is very different; integrating detectors such as CTDs and PDAs have a significant read noise-- the noise introduced by the detector and associated electronics in reading out a single charge packet. The magnitude of the read noise varies from over 1200 electrons for scientific PDAs to under 5 electrons for some low noise CCDs. In CCDs, the sequential transfer of charge from the photosensitive area to a low noise amplifier eliminates the multiplexing circuitry necessary in CIDs and PDAs greatly reducing the capacitance on the amplifier input; therefore, the read noise is extremely low in these devices.

As previously mentioned, the CID detector can measure the charge information nondestructively. Nondestructively reading the CID multiple times and averaging the results decreases the effective read noise of the CID. This technique does not introduce any system or photon noise and hence increases the signal-to-noise ratio (SNR) of a determination. To the extent the read noise is white noise, the effective read noise is decreased as the square root of the number of averaged reads. In practice, the CID read noise is reduced by over an order of magnitude by the process of averaging numerous nondestructive reads (10, 11). The noise observed in current scientific CID systems approaches 1000 electrons but is reducible to under 70 electrons using this method.

CCD detectors also have an imaginative readout mode called binning. Binning is the process of summing the charge contained in multiple elements on

the detector before sensing the total charge (12). The charge in the binned group of detector elements is measured with a single read, and hence has the noise associated with only one read. Binning can be contrasted to summation in computer memory, where the noise associated with reading each element contributes to the overall noise. The advantage of summing the analog signal on-chip using binning as opposed to digital summing in memory is illustrated in Figure 5, which shows the output of a CCD located at the focal plane of a molecular fluorescence instrument (13). In this system, the vertical image of the slit corresponds to 64 rows of the CCD, while the wavelength is displayed in the horizontal dimension. Binning in the slit direction increases the SNR of the spectrum compared to summing in computer memory. Binning in the wavelength direction also increases the SNR of the spectra, albeit at a loss of resolution (4). For low light level spectroscopy, when the dominant source of noise is detector read noise, computer memory summation is noisier by a factor equal to the square root of the number of summed elements as compared to on-detector binning. Figure 5 shows anthracene spectra measured by: (a) reading a single row of the spectrum; (b) reading out all 64 rows and summing in computer memory; and (c) reading the charge information by binning the 64 rows together and reading out this single binned row. As can be seen, the binned mode results in a much higher SNR spectrum.

For low light level spectroscopy, the dark current, or thermal generation of signal, is an important detector parameter directly affecting the maximum observation time. For silicon array detectors, the majority of the thermally generated charge appears at defects in the bulk silicon and at the surface silicon-silicon oxide interface; subsequently, dark current is dependent on

the manufacturing process and geometry. CTDs used in low light level applications are cooled between -30 and -150 °C, so that the dark current is extremely low. However, CCDs cannot be cooled to arbitrarily low temperatures to further reduce the dark current. The ability to transfer the photogenerated charge decreases as the temperature is reduced giving an absolute temperature limit of operation for most CCDs of approximately -150 °C. In a CID, the charge is transferred between electrodes in a single detector element. Thus, they can be operated at lower temperatures since the small amount of charge left behind in one transfer is subsequently collected in the next transfer. Therefore, charge losses are not accumulative as in CCDs. The dark current for properly cooled CCDs is in the range of 0.03 to <0.001 e-/s and for CIDs the dark current is <0.008 e-/s. Dark currents of these levels are insignificant for most analytical spectroscopic applications. Exposures of minutes are required before the dark current is even measurable, and theoretically, exposures of years are required before the devices saturate.

Spectral Responsivity

In many situations, the most important characteristic of an optical radiation detector influencing the SNR of a measurement is the detector quantum efficiency. The intrinsic quantum efficiency of all silicon detectors (PDAs, CTDs, etc.) is high compared to the quantum efficiency of available photoemissive materials in the visible to near-infrared wavelength region. The measured quantum efficiency of silicon detectors varies depending on the structure of the detector (see Table 1). Figure 6 shows the quantum efficiency of representative detectors in the 200-1000 nm wavelength region.

In addition to having a high quantum efficiency in the ultraviolet to the near-infrared regions, some CTDs are able to directly measure photons in the vacuum ultraviolet and the soft x-ray regions (9, 14-15). The quantum efficiency for these high energy photons depends highly on the structure of the detector and the thickness of the overlaying oxide. Quantum efficiencies exceeding 50% have been reported. In addition to x-ray imaging applications, these CTDs can also be used as a direct energy dispersive imaging detector because the measured signal is proportional to the energy of the x-ray photon. On average, one hole-electron pair is created for every 3.65 eV of photon energy. For example, Mn Kα (5.9 KeV) photons produce 1620 e-. The energy resolution of the detector depends on the system read-noise, as well as the ability of the detector to contain all the charge information accurately (i.e. the charge created by a single x-ray event should not be split among neighboring detector elements). For low noise CCDs, the energy resolution obtainable is 150 eV for photon energies >1000 eV. Figure 7 shows an x-ray spectrum obtained using a ^{55}Fe source.

The bandgap of silicon limits the response to photons with wavelengths shorter than ≈1200 nm. Considerable effort has been devoted to extending the longer wavelength range of CTD detectors by making them out of a variety of materials including germanium, indium antimonide and platinum silicide (7,16). The performance of these non-silicon CTDs is expected to improve rapidly. Near- and mid-infrared spectroscopy should greatly benefit with the advent of high quality, low noise multichannel detectors which respond in these regions.

Spectroscopic Characteristics

Low light level spectroscopies such as Raman and luminescence place stringent demands upon a detector system. High responsivity, minimal read noise, and negligible dark current are all necessary for low flux conditions. Figure 8 shows the calculated SNR for the Texas Instruments 800 by 800 CCD and the GE 244 by 388 CID listed in Table 1, as well as a representative photomultiplier tube and photodiode array under low flux conditions. In addition, the SNR for the perfect photon detector is shown, with an assumed 100% QE, zero read noise and no dark current. The only noise source in this curve is the photon shot noise. The comparison shown is for a 10 photons/s illumination level at a wavelength of 600 nm with observation times ranging from zero through one hundred seconds. For the real detectors, these calculations include the effects of photon shot noise, photon flux, detector quantum efficiency, read noise, and dark current shot noise (1). The comparisons are made on a detector element by detector element basis and do not include any multichannel advantages. The photon counting photomultiplier tube used in this comparison has a dark count rate of 5 counts/s, and the photodiode array has a dark count rate of $3*10^4$ e-/s at -20 °C and a read noise of 1200 e-. While almost all commercial PDA systems allow cooling to -20 °C, the dark current of the PDA can be reduced significantly by further cooling. As shown in Figure 8, the CCD has the highest SNR of any of the listed detectors, and is only 11% lower than the perfect photon detector after 100 seconds. The sensitivity of CCDs has long been exploited by astronomers (17-19), and is beginning to be recognized by researchers in other fields (13, 20-22).

The ability of a detector to measure photon fluxes varying over a wide range is important in spectroscopic applications. The range of photon fluxes that the detector is able to quantify depends on a number of parameters, both detector related (such as maximum readout rate, maximum integration time, read noise and dark current) and system dependent (such as the number and relative intensities of the spectral features, maximum observation time, source drift). These detectors have a simple dynamic range defined as the ratio of the maximum amount of charge that can be contained in a detector element to the minimum amount of charge that can be measured. The simple dynamic range of some modern CCDs approaches one million, large enough for many spectroscopic applications.

In some areas of spectroscopy, the ability to measure faint spectral lines in the presence of bright spectral features is important. The intense features should not influence the quantitation of the weak features. Some CTDs can suffer from problems when the charge storage ability of a detector element is exceeded. After the charge capacity of an individual CTD detector is reached, additional charge can spill into nearby detector elements in a process called blooming. Charge which blooms from a detector element exposed to a high photon flux can mask the signal of nearby elements. There are several methods used to alleviate blooming in CTDs. In CIDs, the excess charge is transferred into the substrate. In addition, some CCDs are fabricated with anti-blooming structures.

CIDs allow a means of extending their effective dynamic range using a process called random access integration in which the actual integration times are varied during a given experiment from detector element to element based on the amount of light reaching each element. In practice, this is achieved by

scanning through the device, reading each detector element nondestructively, and determining the signal level at each element. A decision determining optimum integration time is based on the observed photon flux. Quantitation is achieved by storing the observed signal and integration time. Using this method, strong lines are integrated for short periods, while weak features are allowed to integrate until sufficient SNR is obtained. In atomic emission spectroscopy, dynamic ranges exceeding seven orders of magnitude have been quantified using the random access integration time technique with CID detection (11).

Conclusions

CIDs and CCDs have great potential to solve challenging spectroscopic problems. CTDs offer negligible dark currents, peak quantum efficiencies over 80%, low read noises and wide dynamic ranges. In addition, the ability of CCDs to bin photogenerated charge from multiple elements and the nondestructive readout mode of CIDs contribute to the flexibility these detectors offer to the spectroscopist. The availability of these detectors from several manufacturers in a large variety of formats and sizes which respond over a wide wavelength range gives considerable choice in a detector. While the application of this technology to analytical spectroscopy has been slow, CTDs are currently being used with impressive results. The second article in this series describes the use of CTD detectors to overcome a variety of difficult analytical problems. Future applications of CTDs will continue to broaden the utility and increase the performance of many areas of spectroscopy.

Acknowledgements

The authors thank James R. Janesick of Jet Propulsion Laboratory for use of the ^{55}Fe x-ray spectrum, Richard Aikens of Photometrics Ltd., Tucson, AZ, and Phillip Miller of Lawrence Livermore National Laboratory.

Credits

This article is based upon work partially funded by the Office of Naval Research, and Smith Kline Beckman.

References:

1) Bilhorn, R.B.; Sweedler, J.V.; Epperson, P.M.; Denton, M.B. Applied Spectroscopy, 1987, 41(7), 1114.

2) Bilhorn R.B., Epperson P.M., Sweedler J.V. and Denton M.B., Applied Spectroscopy ,1987, 41(7), 1125.

3) Sims, G.R.; Denton, M.B. In Multichannel Image Detectors, Talmi, Y., Ed.; ACS Symposium Series No. 236, 1983; Vol.2, Chap. 5.

4) Denton, M.B.; Lewis, H.A.; Sims, G.R. In Multichannel Image Detectors, Talmi, Y., Ed.; ACS Symposium Series No. 236, 1983; Vol 2., Chap. 6.

5) See the Journal of Optical Engineering 26, Nos. 8,9,10 (1987).

6) Janesick, J.R.; Elliott, T.; Collins, S.; Marsh, H.; Blouke, M.; Freeman, J. In State-of-the-Art Imaging Arrays and their Applications, Prettjohns, K., Ed.; Proc. SPIE, 1984, 501, 2.

7) Dereniak, E.L.; Crowe, D.G. Optical Radiation Detectors; John Wiley, New York, 1984.

8) Epperson, P.M.; Sweedler, J.V.; Denton, M.B.; Sims, G.R.; McCurnin, T.W.; Aikens, R.S. J. Opt. Eng., 1987, 26, 715.

9) Janesick, J.R.; Elliott, T.; Collins, S.; Blouke, M.M.; Freeman, J. J. Opt. Eng., 1987, 26, 692.

10) Sims, G.R; Denton, M.B. J. Opt. Eng., 1987, 26, 1008.

11) Bilhorn, R.B. Ph.D. Dissertation, University of Arizona, August 1987.

12) Epperson, P.M.; Denton, M.B. Analytical Chemistry, 1987, submitted 11/87.

13) Epperson, P.M.; Jalkian, R.D.; Denton, M.B. in preparation.

14) Stern, R.A.; Liewer, K.; Janesick, J.R. Rev. Sci. Instrum., 1983, 54, 198.

15) Janesick, J.R.; Campbell, D.; Elliott, T.; Daud, T.; Ottley, P. In UV Technology, Huffman, R., Ed., Proc. SPIE, 1986, 687, 36.

16) See the Journal of Optical Engineering 26, No 3 (1987).

17) Oke, J.B. In Solid State Imagers for Astronomy, Geary, J.C. and Latham, D.W., Eds.; Proc. SPIE, 1981, 290, 45.

18) Goad, L.E. In Instrumentation in Astronomy IV, Crawford, D.L., Ed.; Proc. SPIE, 1981, 331, 130.

19) York, D.G.; Jenkins, E.B.; Zucchino, P.;Lowrance, J.L.; Long, D.: Songaila, A. In Solid State Imagers for Astronomy, Geary, J.C. and Latham, D.W., Eds.; Proc. SPIE, 1981, 290, 202.

20) Murray, C.A.; Dierker, S.B. J. Opt. Soc. Am. A, 1986, 3, 2151.

21) Strauss, M.G.; Naday, I.; Sherman, I.S.; Zaluzec, N.J. Ultramicroscopy, 1987, 22, 117.

22) Hiraoka, Y.; Sedat, J.W.; Agard, D.A., Science 1987, 238, 36.

Table I. Characteristics of Selected CTDs

Device	Architecture	Dimensions (elements)	Photoactive Area (mm)	Peak QE (%) wavelength	Range over which QE exceeds 10%	Charge Capacity (electrons)	Read Noise (electrons)
General Electric CID17-B	CID	244 by 388	6.5 by 8.7	47% at 500 nm	210 - 850 nm	$6x10^5$	60
General Electric CID75	CID	1 by 1	1.0 by 1.0	35% at 250 nm	200[1] - 850 nm	$1x10^6$	80
Kodak M1A	Frontside CCD	1035 by 1320	7.0 by 9.0	37% at 700 nm	450 - 900 nm	$4x10^4$	10
Reticon	Frontside CCD	404 by 128	21.0 by 6.6	NA	420 - 1000 nm	$2x10^6$	45
RCA SID501EX	Backside CCD	512 by 320	15.4 by 9.6	90% at 500 nm	200[1] - 950 nm[2]	$4x10^5$	50
Tektronix TK512M-011	Frontside CCD	512 by 512	13.8 by 13.8	35% at 750 nm	450 - 950 nm	$9x10^5$	6
Texas Instruments	Backside CCD	800 by 800	12.0 by 12.0	90% at 550 nm	0.1[1] - 1000 nm[2]	$5x10^4$	7
Texas Instruments TC104-1	Frontside CCD	3456 by 1	35.6 by .01	90% at 400 nm	200[1] - 950 nm	$3x10^5$	80
Thomson-CSF TH7882CDA	Frontside CCD	384 by 576	8.8 by 13.2	45% at 650 nm	420 - 950 nm	$5x10^5$	10

[1] Point at which QE measurements stopped. QE may exceed 10% beyond this point.
[2] Detectors received additional processing.

Figure Captions

Figure 1:

Cross section of a hypothetical CTD detector element when the electrodes are biased for charge integration. The absorption of a photon causes hole/electron formation, and the positively charged hole is collected under the negatively charged electrode.

Figure 2:

Layout of a typical three-phase CCD. Photogenerated charge is shifted from the imaging area in parallel to the serial register (down in figure). The charge in the serial register is then shifted left to the on-chip amplifier and measured.

Figure 3:

Hypothetical CID array detector showing the sense and collection addressing shift registers. The registers open and close a series of switches to connect the collection and sense capacitor electrodes to the charge drive signal and output amplifier. The detector element at the intersection of the selected sense and collection capacitors is shaded.

Figure 4:

Photograph showing many of the charge transfer device detectors available over the last few years. The number of detector elements range from one to over four million, and the photoactive areas range from under 0.2 mm^2 to over 3000 mm^2. Photograph courtesy of Photometrics Ltd., Tucson AZ.

Figure 5:

Fluorescence spectra of anthracene obtained with a CCD detector. The slit image illuminates 64 rows of the CCD. (A) - (C) show the results of three methods of reading out the CCD with each spectra scaled for comparison. (A) The anthracene spectrum obtained from reading only one of the 64 illuminated rows of the CCD. (B) The result of reading out and summing in computer memory all 64 rows of the slit image. The resulting spectrum has approximately 8 times the SNR of the spectrum in (A). (C) The output of the CCD when the photogenerated charge from all 64 rows is binned into a single row, and the single binned row is read. The spectrum in (C), while having the same absolute signal as in (B), has approximately 64 times the SNR of the spectrum in (A).

Figure 6:

Quantum efficiency of several representative detectors; a Texas Instruments 800 by 800 CCD (9), a General Electric 244 by 388 CID, a Reticon RL1024S PDA, and a Hammamatsu GaAs opaque photocathode available in PMTs.

Figure 7:

X-ray spectrum of a ^{55}Fe x-ray source using a CCD as an energy dispersive detector showing the Mn Kα and Mn Kβ lines, as well as both escape peaks and the silicon absorption peak. The Ag Lα peak is from Ag impurity in the source. The peak energy is obtained by multiplying the signal by a factor combining the CCD gain of 0.8 e-/DN and the 3.65 eV of photon energy per electron produced (2.92 eV/DN). Spectrum courtesy of J. R. Janesick, Jet Propulsion Laboratory (9).

Figure 8:

Calculated performance curves for the same detectors as in Figure 5 showing the SNR obtained with a photon flux of 10 photons/s for observation times ranging from 0 to 100 s at a wavelength of 600 nm. The top curve is for the perfect photon detector with 100% quantum efficiency and no noise sources except photon shot noise (the uncertainty caused by the random arrival of photons to the detector). The model used in these calculations includes the effects of photon shot noise, detector read noise, detector quantum efficiency, and detector dark current. See text for other detector characteristics.

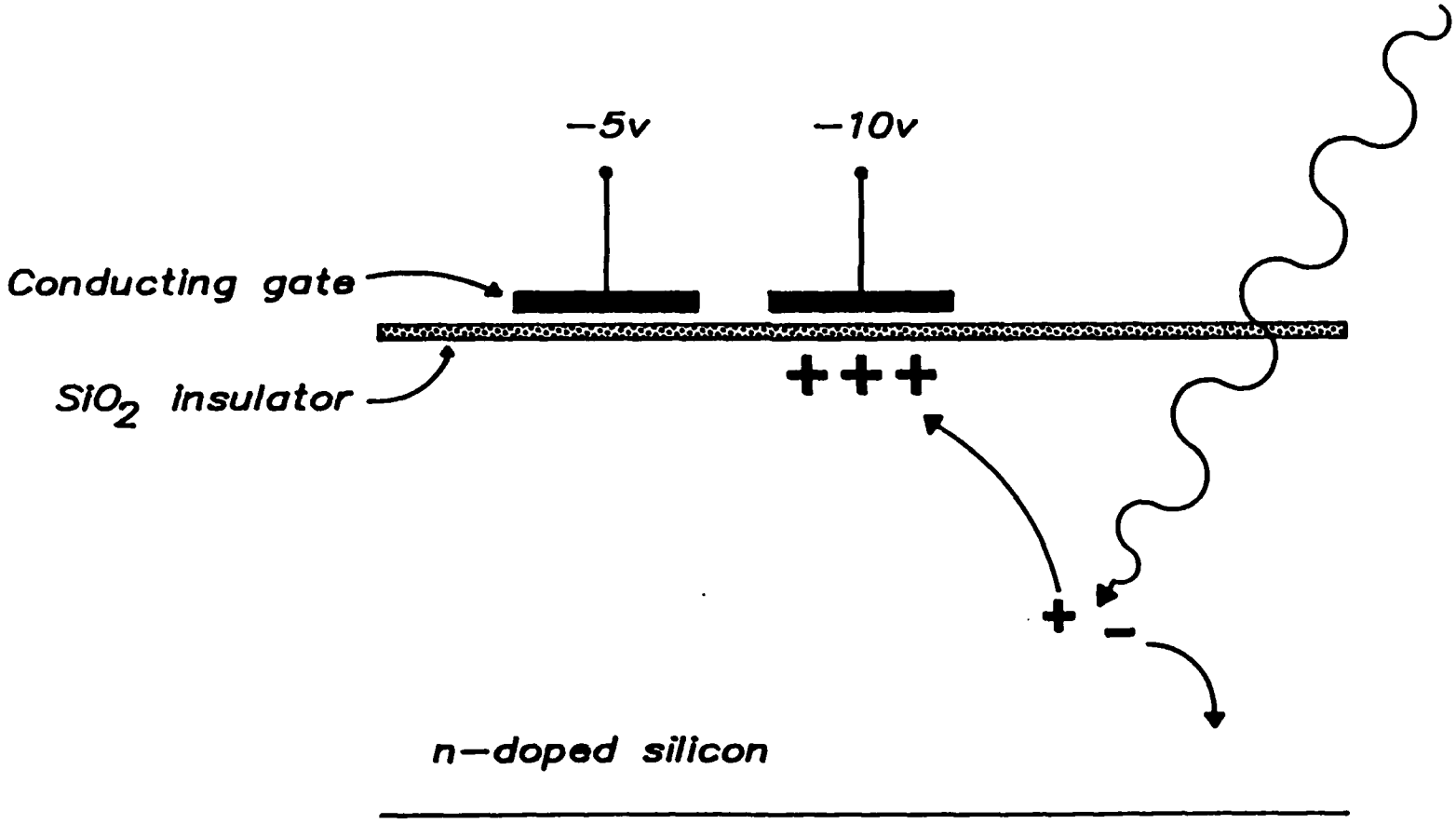

FIGURE 1

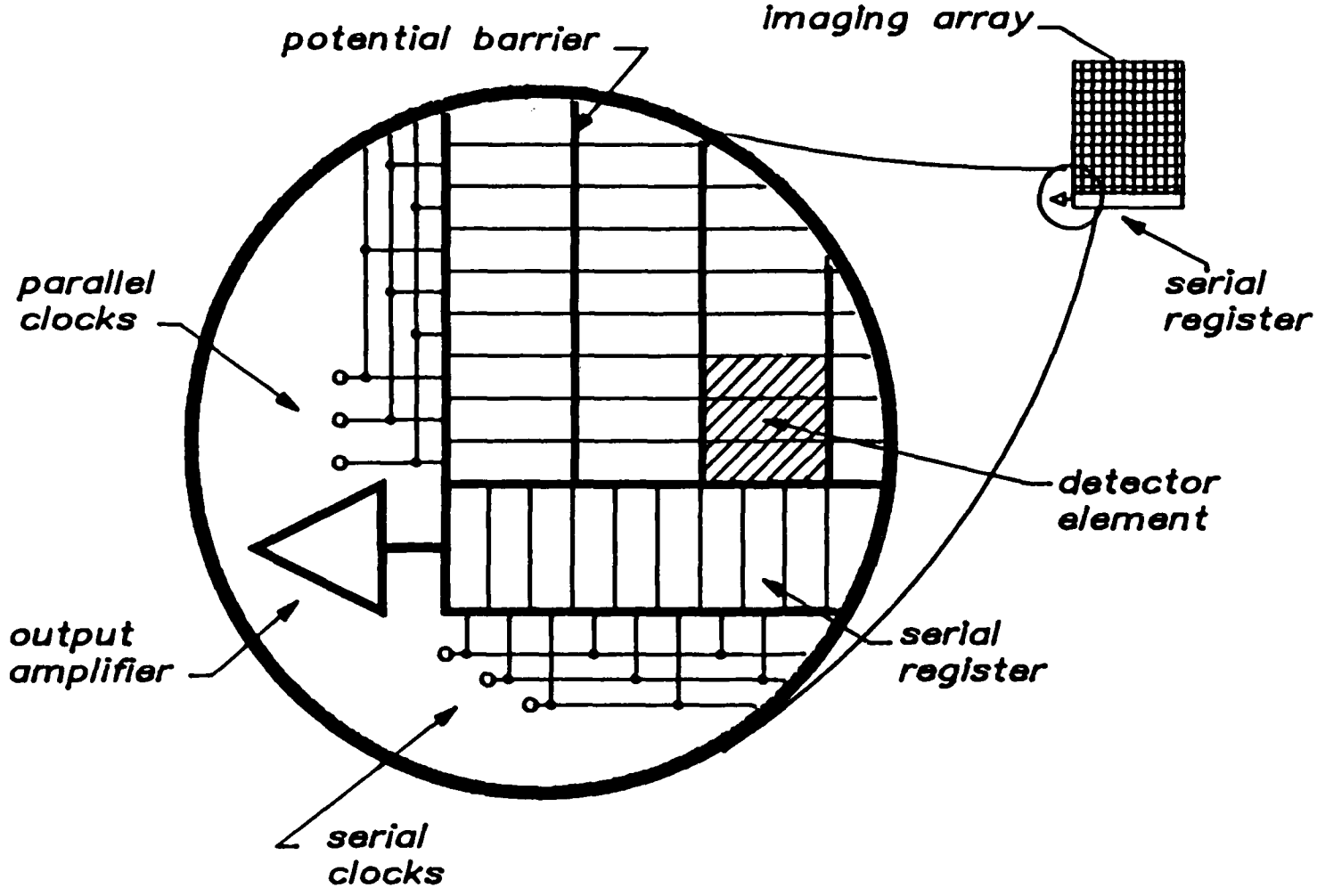
potential barrier
imaging array
parallel clocks
serial register
detector element
output amplifier
serial register
serial clocks

FIGURE 2

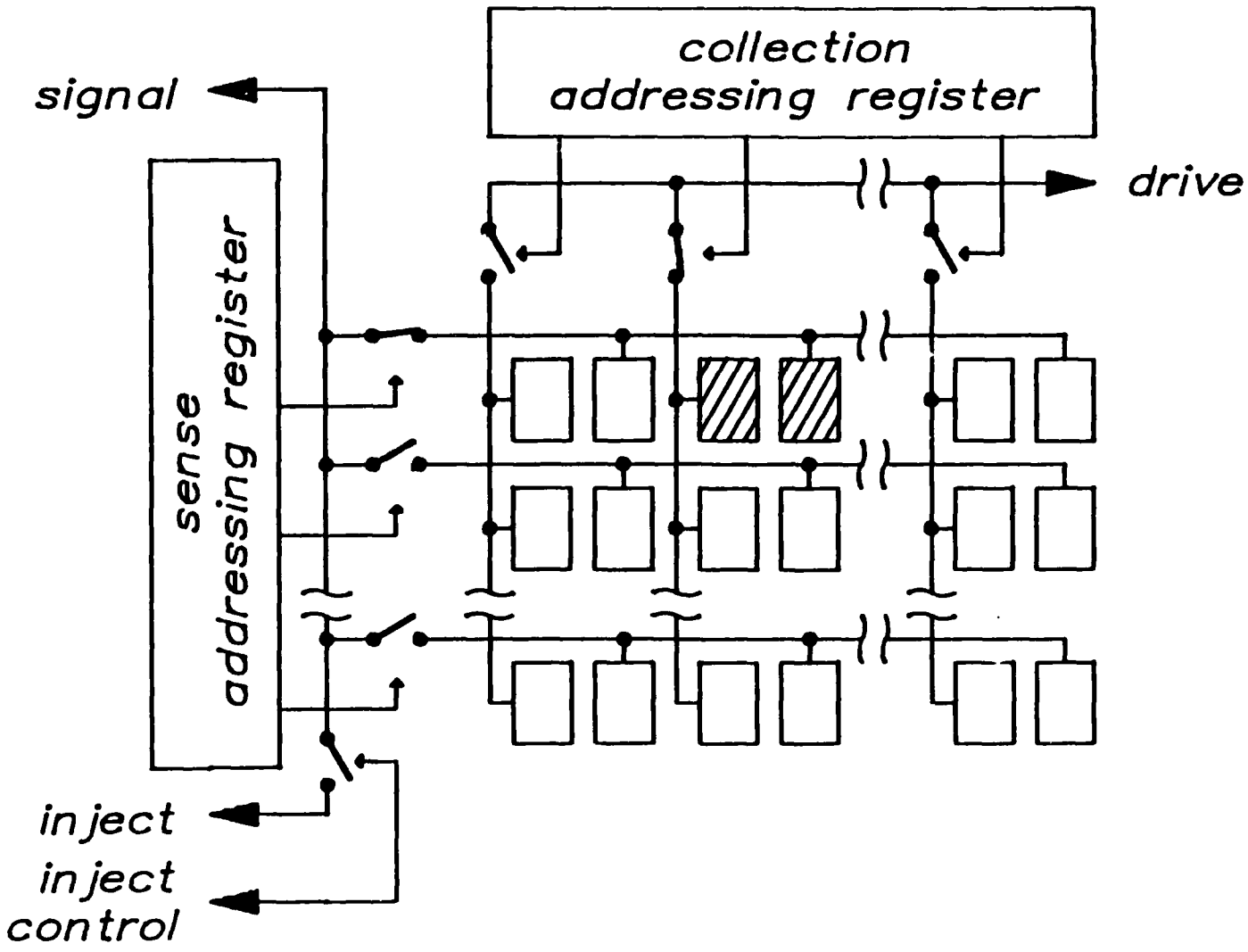
collection
addressing register
signal
drive
sense
addressing register
inject
inject
control

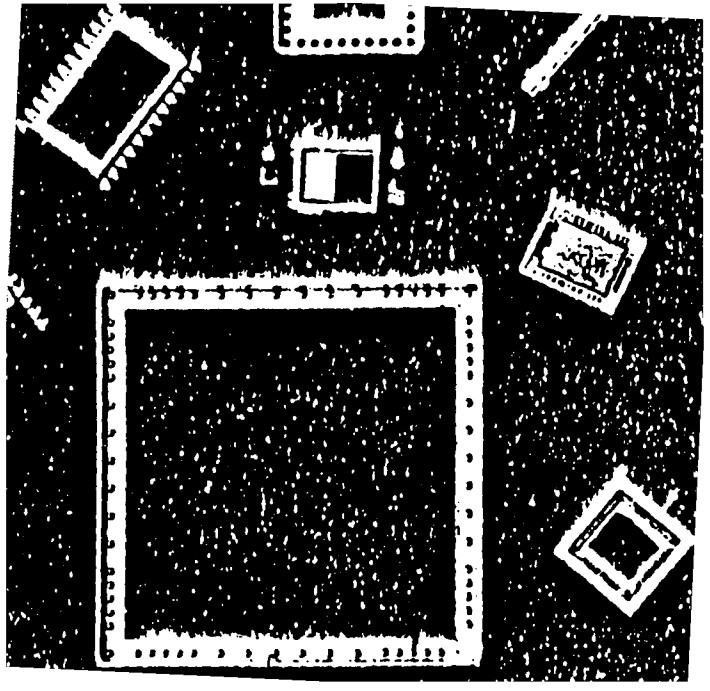

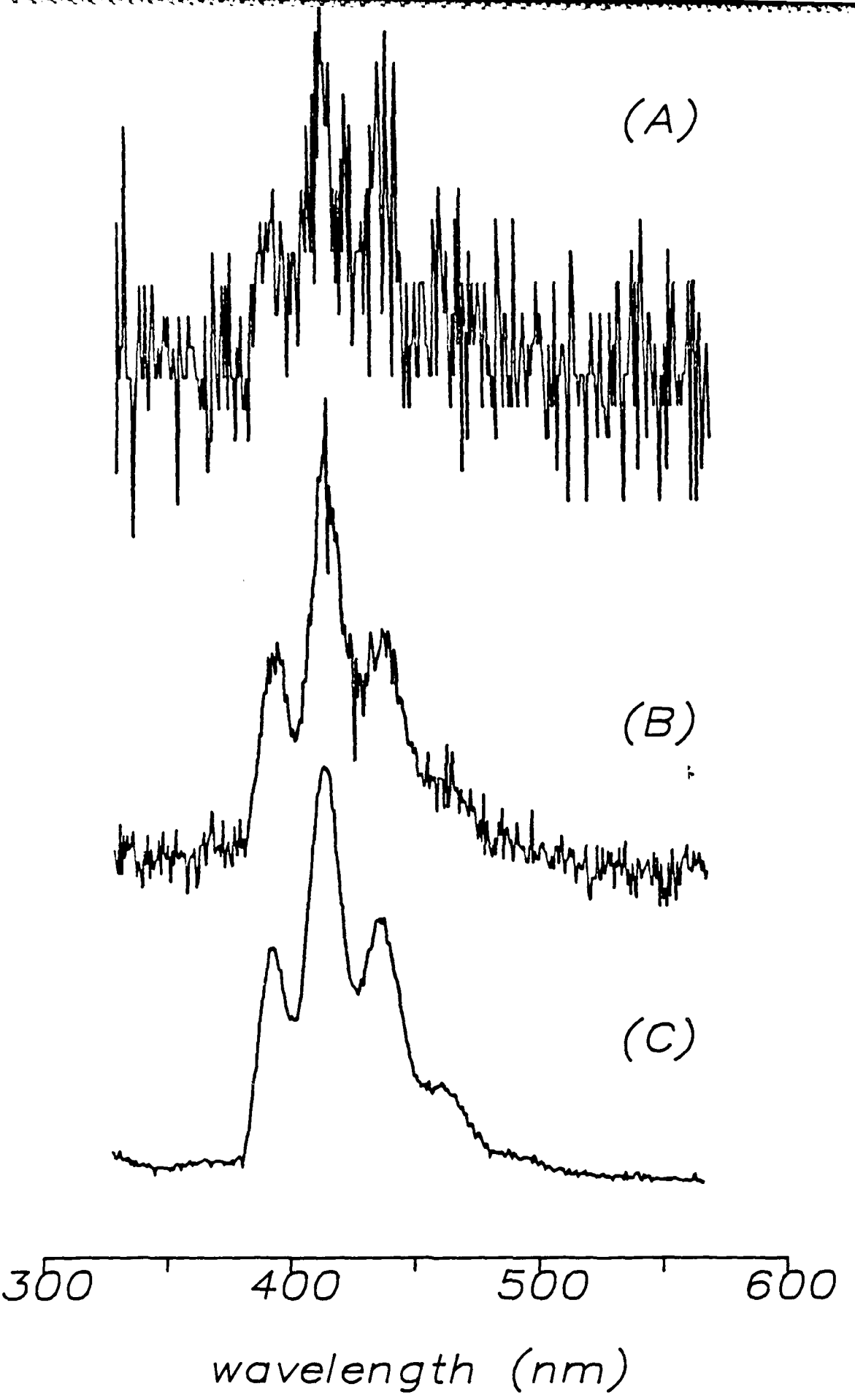

FIGURE 5

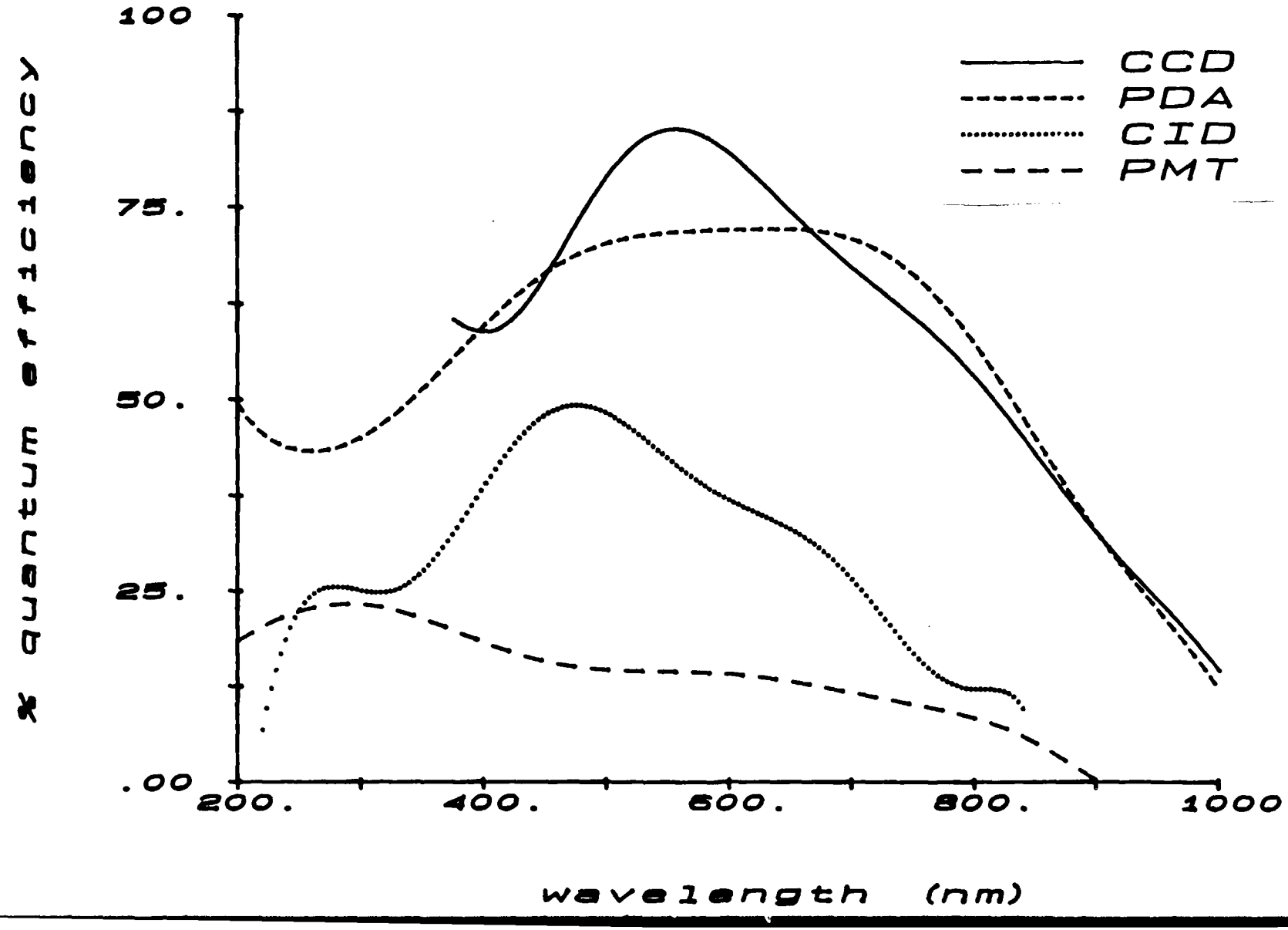
100
75.
50.
25.
.00
% quantum efficiency
200.
400.
600.
800.
1000
wavelength (nm)
CCD
PDA
CID
PMT

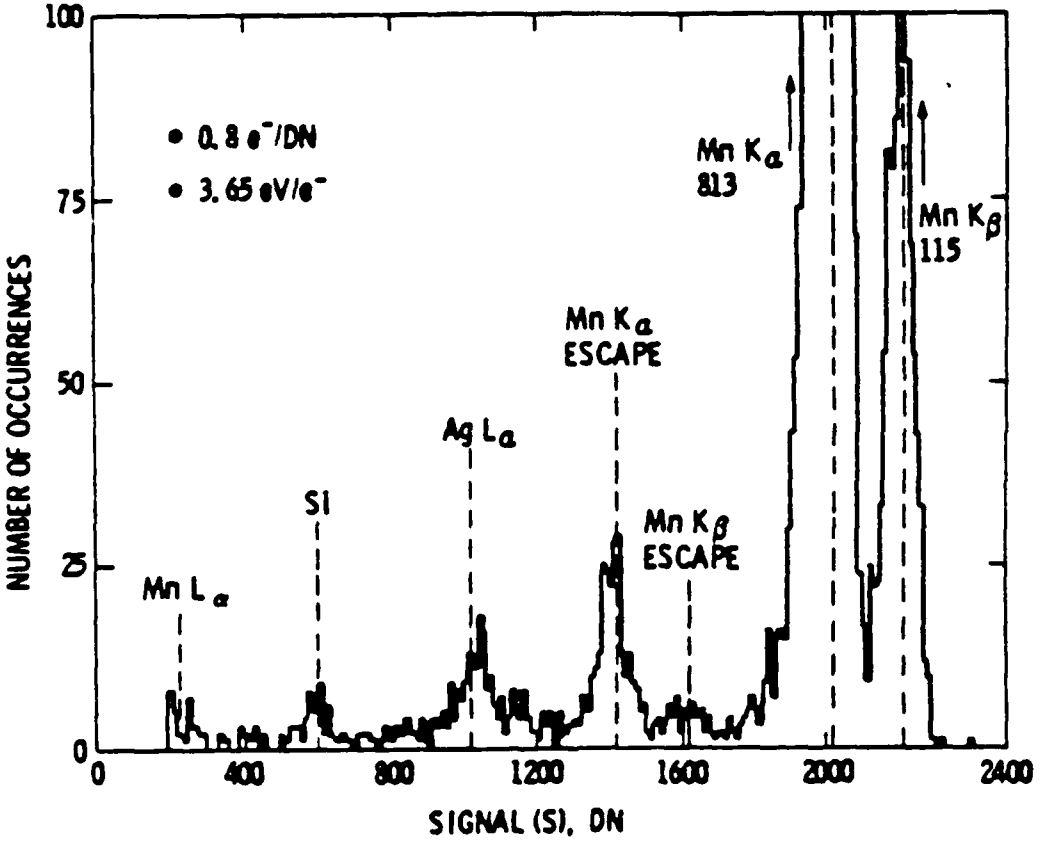
100
75
50
25
0
NUMBER OF OCCURRENCES
• 0.8 e⁻/DN
• 3.65 eV/e⁻
Mn Kα
813
Mn Kβ
115
Mn Kα
ESCAPE
Ag Lα
Si
Mn Kβ
ESCAPE
Mn Lα
0
400
800
1200
1600
2000
2400
SIGNAL (S), DN

FIGURE 7

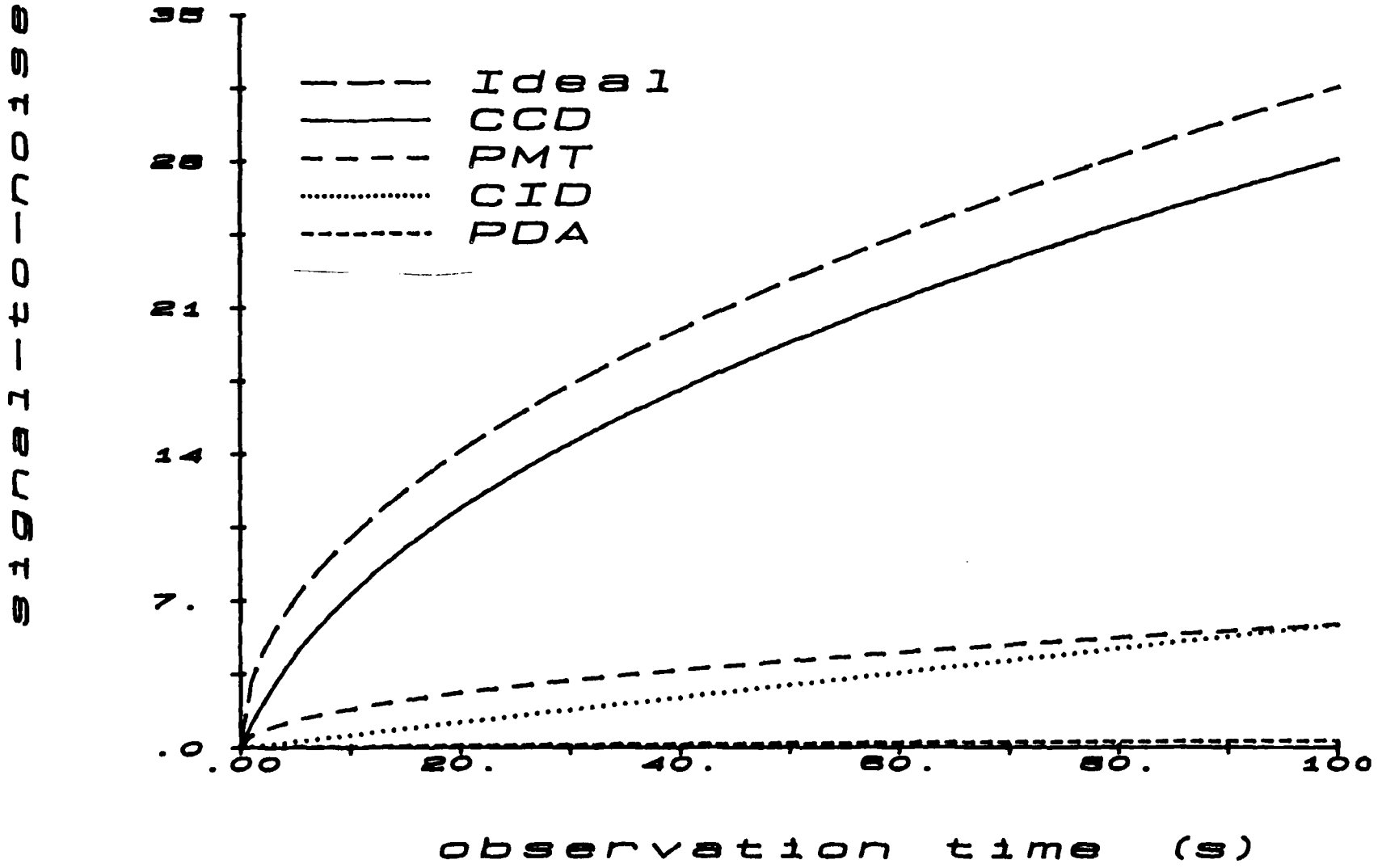
signal-to-noise
35
28
21
14
7.
.0
.00
20.
40.
60.
80.
100
observation time (s)
Ideal
CCD
PMT
CID
PDA

DL/1113/87/2

TECHNICAL REPORT DISTRIBUTION LIST, GEN

	No. Copies
Office of Naval Research Attn: Code 1113 800 N. Quincy Street Arlington, Virginia 22217-5000	2
Dr. Bernard Douda Naval Weapons Support Center Code 50C Crane, Indiana 47522-5050	1
Naval Civil Engineering Laboratory Attn: Dr. R. W. Drisko, Code L52 Port Hueneme, California 93401	1
Defense Technical Information Center Building 5, Cameron Station Alexandria, Virginia 22314	12 high quality
DTNSRDC Attn: Dr. H. Singerman Applied Chemistry Division Annapolis, Maryland 21401	1
Dr. William Tolles Superintendent Chemistry Division, Code 6100 Naval Research Laboratory Washington, D.C. 20375-5000	1
Dr. David Young Code 334 NORDA NSTL, Mississippi 39529	1
Naval Weapons Center Attn: Dr. Ron Atkins Chemistry Division China Lake, California 93555	1
Scientific Advisor Commandant of the Marine Corps Code RD-1 Washington, D.C. 20380	1
U.S. Army Research Office Attn: CRD-AA-IP P.O. Box 12211 Research Triangle Park, NC 27709	1
Mr. John Boyle Materials Branch Naval Ship Engineering Center Philadelphia, Pennsylvania 19112	1
Naval Ocean Systems Center Attn: Dr. S. Yamamoto Marine Sciences Division San Diego, California 91232	1

END
DATED
FILM
8—88
DTIC